



# Molecular Clouds resolved with ALMA $^{12}\text{CO } J=1-0$ and $J=2-1$ observations towards the Magellanic Bridge

M.T. Valdivia<sup>1</sup>, M. Muñoz<sup>1</sup>, M. Rubio<sup>1</sup> & H. Saldaño<sup>2</sup>

<sup>1</sup> *Departamento de Astronomía, Universidad de Chile, Santiago, Chile*

<sup>2</sup> *Observatorio Astronómico de Córdoba, UNC, Argentina*

Contact / maria.valdivia@ug.uchile.cl

**Resumen** / Presentamos los resultados de observaciones de  $^{12}\text{CO } J = 1 - 0$  y  $J = 2 - 1$ , hechas con el interferómetro ALMA para las regiones B y C del Puente de Magallanes. La resolución de los datos provenientes de ALMA nos permite resolver nubes moleculares: la región B consta de al menos 5 nubes, con radios equivalentes que varían de 2 a 4.5 pc; la región C está compuesta de 7 nubes con radios equivalentes entre 0.5 y 2.5 pc. Todas estas nubes moleculares tienen perfiles de velocidad muy angostos ( $\Delta v = 0.7 - 1.8 \text{ km s}^{-1}$ ), indicando la presencia de gas frío. Las razones de línea son todas cercanas a 1 (varían entre 0.8 a 1.4), lo que es consistente con nubes densas y ópticamente gruesas. Estas fuentes siguen las mismas tendencias en sus propiedades físicas que otras nubes de baja metalicidad en el Grupo Local, incluyendo las Nubes de Magallanes.

**Abstract** / We present the results of the ALMA  $^{12}\text{CO } J = 1 - 0$  and  $J = 2 - 1$  observations done in regions B and C of the Magellanic Bridge. The resolution of ALMA data allows us to identify individual molecular clouds: region B is resolved into at least 5 clouds with radii spanning from 2 to 4.5 pc and region C consists of 7 clouds with radii from 0.5 to 2.5 pc. All of these have narrow velocity line widths ( $\Delta v = 0.7 - 1.8 \text{ km s}^{-1}$ ), which indicate very cold and quiescent gas. We also found that the line ratios are all close to 1 (ranging from 0.8 to 1.4) consistent with optically thick and dense clouds. These sources follow the same tendencies in their physical properties than other dwarf galaxies of the Local Group, including the SMC and LMC.

*Keywords* / ISM: clouds — ISM: molecules — Magellanic Clouds

## 1. Introduction

The Magellanic Bridge was first recognized by Hindman et al. (1963), through 21 cm observations of HI. With an extension between 15 to 21 kpc wide, it is thought that it was caused by a close interaction between the Large Magellanic Cloud (LMC) and the Small Magellanic Cloud (SMC) around 200 Myrs ago (Gardiner et al., 1994). It is the closest tidally interacting system, at around 60 kpc from the Sun (Harries et al., 2003), and it has a metallicity of  $Z_{\odot}/5 - Z_{\odot}/10$  (Lehner et al., 2008). The first detection of a carbon monoxide (CO) bright source in the Bridge was made by Muller et al. (2003), using measurements of the  $^{12}\text{CO } J = 1 - 0$  rotational transition. Based on this and coincidences of HI and  $100 \mu\text{m}$  emission, Mizuno et al. (2006) found seven more sources using the NANTEN telescope. These have narrow velocity profiles (linewidths smaller than  $2 \text{ km s}^{-1}$ ), low integrated CO brightnesses ( $10$  to  $140 \text{ mK km s}^{-1}$ ) and are associated with young stellar objects (Chen et al., 2014).

In this work, we focus on the sources labeled as Magellanic Bridge B and C (MagBridgeB and MagBridgeC). Individual clouds can be resolved due to the enhanced resolution of the line emission data obtained with the Atacama Large Millimeter/Submillimeter Array (ALMA) interferometer. We compare the molecular clouds in this metal-poor region with others found in metal-poor galaxies of the Local Group and in the Milky

Way, using for this purpose the virial mass vs. CO luminosity and the relation known as Larson's law, which relates velocity dispersion and size ( $\sigma_v \propto S^{\alpha}$ ) (Larson, 1981).

## 2. Data

Observations for the  $^{12}\text{CO } J = 1 - 0$  and  $J = 2 - 1$  were carried out by the ALMA telescope during Cycle 3: the  $J = 1 - 0$  line cube was carried out in band 3 using the main array 12m antennas, with a rest frequency of 115.2 GHz, and the  $J = 2 - 1$  line cube, in band 6 using the Atacama Compact Array (ACA) 7 m antennas at a rest frequency of 230.8 GHz.

The reduction and cleaning of the data was done using Common Astronomy Software Applications (CASA). The properties of the cubes are in Table 1. Also, the line cubes were integrated through the velocity axis between 140 and  $149 \text{ km s}^{-1}$  for MagBridgeB and 175 and  $182 \text{ km s}^{-1}$  for MagBridgeC. The rms of this integration is also in Table 1.

The clouds were identified using the following procedure over the  $J = 1 - 0$  data: the rms of the integrated image was taken, and using a contour map set at  $3\sigma$  over the image, the area covered by each cloud was determined. Then, using the line cube and the contours, we obtained the mean spectra of each source with CASA, which we used to estimate the center, peak temperature, and FWHM of each cloud. This procedure does

Table 1: Properties of the images, given by region and emission line. The rms is calculated for the integrated images.

	MagBridgeB		MagBridgeC	
Line	1-0	2-1	1-0	2-1
Beam major ["]	3.3	6.9	3.6	6.6
Beam minor ["]	2.5	6.0	3.3	5.7
$\Delta v$ [km s <sup>-1</sup> ]	0.5	0.16	0.5	0.5
rms [Jy beam <sup>-1</sup> km s <sup>-1</sup> ]	0.11	1.23	0.23	1.26

not recognize clouds that have a different structure in the velocity axis, but only separates clouds if they can be spatially resolved.

To compare the emission of both rotational transitions, first we convolved the  $J = 1 - 0$  integrated image and line cube to the same resolution of the corresponding  $J = 2 - 1$  map for each source (B and C). Afterwards, we obtained the  $3\sigma$  contours for the  $2 - 1$  transition image and used those contours to obtain a mean spectra of each source, for each rotational transition.

### 3. Results

#### 3.1. Detection of molecular clouds

In the  $^{12}\text{CO}(1-0)$  ALMA cubes, we detected 5 molecular features for source B (labeled from 1 to 5) and 7 for source C (labeled from 1 to 7), all with signal-to-noise over 10. The integrated moment map, with the identified regions, is in Fig. 1 for MagBridgeB and C. Almost all are separated by at least one beam size, except for regions 4 and 5 of MagBridgeC: their angular distance (around 3") is slightly less than the semi-major axis size of the beam area, so after convolution with the  $\text{CO}(2-1)$  beam, they are considered to be the same region.

From a comparison between the molecular features observed in the  $J = 1 - 0$  transition with those observed in the  $J = 2 - 1$  line, it can be appreciated that they coincide spatially and in velocity range.

#### 3.2. Physical properties of the molecular clouds

We have derived the radii, luminosities and virial and  $\text{H}_2$  masses for each of the clouds based on the  $J = 1 - 0$  line cube. The radii  $R_{eq}$  are calculated approximating each source as a spherical cloud and obtaining the projected area ( $\pi R_{eq}^2$ ). For this, we assume that the Magellanic Bridge is at a similar distance from us as the SMC (63 kpc away, Harries et al. 2003). The virial mass  $M_{vir}$  was calculated using equation 3 of MacLaren et al. (1988): we used a value of  $k_2 = 190$  for a density distribution of  $\rho(r) \propto r^{-1}$ . The CO luminosity  $L_{CO}$  was calculated in  $\text{K km s}^{-1} \text{pc}^2$  using:

$$L_{CO} = 2453 S_{CO} \Delta V D_L^2 \quad (1)$$

where  $S_{CO} \Delta V$  is the integrated flux density in  $\text{Jy km s}^{-1}$  and  $D_L$  is the luminosity distance in Mpc (Bolatto et al., 2013). Only for comparison, we calculate the  $\text{H}_2$  mass (molecular mass)  $M_{mol}$  using the galactic  $\text{H}_2$  mass to CO luminosity factor  $\alpha_{CO} = 4.3 M_{\odot} (\text{K km s}^{-1} \text{pc}^2)^{-1}$ ,

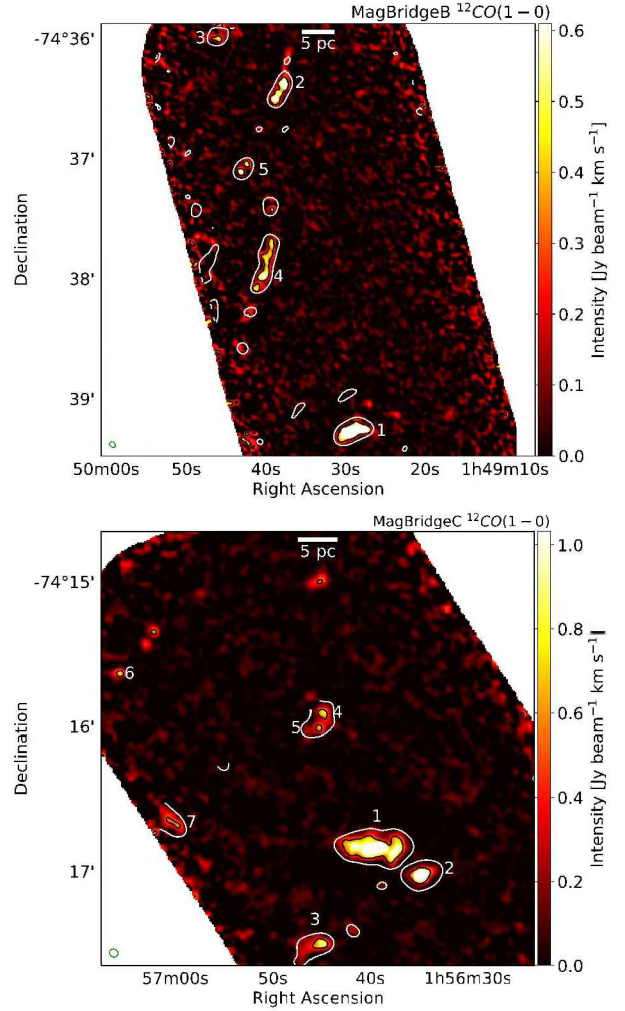


Figure 1:  $J = 1 - 0$  integrated moment maps for MagBridgeB and C. Black contours are  $3\sigma$  level for  $J = 1 - 0$  integrated moment map and green ellipses on the bottom left corners are the beam sizes. The identified clouds are labeled with white numbers. White contours correspond to  $3\sigma$  level for  $J = 2 - 1$  integrated moment map. Top: MagBridgeB. Bottom: MagBridgeC.

$^{-1}$ , which assumes a CO-to- $\text{H}_2$  conversion factor  $X_{CO}$  of  $1 \times 10^{20} \text{ cm}^{-2} (\text{K km s}^{-1})^{-1}$ .

The ranges for each of these parameters for the whole sample is in Table 2. The narrow CO emission ( $\Delta v \lesssim 2 \text{ km s}^{-1}$ ) indicates very cold and (probably) inactive gas. There is a tendency for the virial mass to be at least 5 times greater than the molecular mass, calculated using the galactic value. This implies that the CO-to- $\text{H}_2$  conversion factor in this region needs to be higher, in agreement with the suggestion that the conversion factor increases with decreasing metallicity (Bolatto et al., 2013).

We compare our data with other metal-poor molecular clouds (Rubio et al., 2015) and galactic plane clouds, which have a power law exponent  $\alpha$  of 0.5 for Larson's law and 0.81 for mass vs. luminosity (Solomon et al., 1987). We plot data from Bolatto et al. (2008), Wong et al. (2011), Rubio et al. (2015) and Schrubba et al. (2017)

Table 2: Ranges for the physical parameters calculated for the clouds using CO(1-0) data.  $R_{eq}$  and  $\Delta v$  are taken directly from the data, whereas the mass, luminosity and line ratios are derived.

Cloud	$\Delta v$ [km s <sup>-1</sup> ]	$R_{eq}$ [pc]	$M_{vir}$ [ $M_{\odot}$ ]	$L_{CO}$ [K km s <sup>-1</sup> pc <sup>2</sup> ]	$M_{mol}$ [ $M_{\odot}$ ]	$R_{CO(2-1)/CO(1-0)}$
B	0.3 - 0.8	1.9 - 4.5	349 - 2578	3.7 - 106.0	16 - 456	0.82 - 1.36
C	0.3 - 0.7	0.5 - 2.5	91 - 984	3.9 - 137.7	17 - 592	0.86 - 1.96

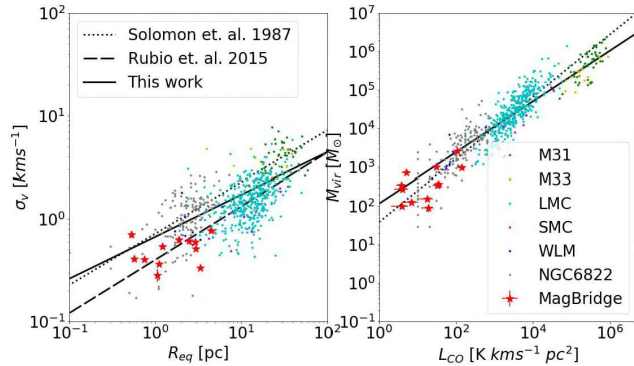


Figure 2: Correlations of molecular clouds in dwarf galaxies within the Local Group. Red stars correspond to the data in this work. Dotted lines mark the relations for the Milky Way molecular clouds. The dashed line corresponds to the relation for dwarf galaxies (Rubio et al., 2015) excluding the MagBridge (this work) and NGC 6822 (Schruba et al., 2017). The solid line is a fit to all points (this work). Left:  $R_{eq}$  vs.  $\sigma_v$ . Right:  $L_{CO}$  vs.  $M_{vir}$ .

for dwarf galaxies, which are shown in Fig. 2. Our work complements the small size and low-luminosity edge of these relations and in general, our data correlate with other metal-poor clouds. Using Maximum Likelihood and Markov Chain Monte Carlo (MCMC), we fit the best line that correlates them all. A power law fit gave us an exponential index of 0.41 for Larson’s law, similar to the indexes (0.5 and 0.52) found by Solomon et al. (1987) and Rubio et al. (2015) respectively, and of 0.66 for virial mass vs. luminosity, lower than the index for galactic plane clouds. This indicates that the clouds found are close to virial equilibrium and the differences in the power laws can be a result of lower metallicity.

### 3.3. Line Ratios

We define the line ratio as the ratio between the peak temperature of the spectra, in Kelvin, for both transitions:

$$R_{\frac{CO(2-1)}{CO(1-0)}} = T_{CO(J=2-1)} / T_{CO(J=1-0)} \quad (2)$$

A ratio close to 1 in Eq. 2 is consistent with optically thick clouds (Eckart et al., 1990).

In both regions studied, most of the clouds have line ratios close to 1, as seen in Table 2. The coldest clouds in each region have the smallest ratios (cloud 4 in MagBridgeB and cloud 3 in MagBridgeC). At the same time, those with the greatest ratio (cloud 1 in MagBridgeB and cloud 4 in MagBridgeC) are probably the hottest. Also, there are no line ratio gradients within the clouds, which show that there are no important temperature gradients within them.

BAAA 61A (2019)

## 4. Conclusions

We study two regions of the Magellanic Bridge where, due to the enhanced ALMA resolution, two previous CO detections could be resolved into 12 individual molecular clouds. In general, the clouds have equivalent radii smaller than 5 pc, narrow velocity profiles consistent with cold and quiescent gas and line ratios consistent with optically thick gas. These clouds are smaller than other recently reported ones in metal-poor dwarf galaxies and follow the same trends in size vs. velocity dispersion and mass vs. luminosity. These relations suggest that these clouds are in an approximate virial equilibrium. Other relations (like velocity dispersion vs. virial mass and column density vs. luminosity) will be studied as future work.

*Acknowledgements:* We would like to thank the editor of the BAAA R. Gamen and the anonymous referee for their useful comments that helped to improve this article. M.T.V. wishes to acknowledge support from CONICYT-PFCHA/ Magister Nacional/2018 - 22180279 and support from SOCHIAS grant through ALMA/CONICYT project #31160034. M.R. wishes to acknowledge support from ENLACE-FONDECYT project ENL22/18, Universidad de Chile, FONDECYT grant no.1140839 and partial support through project BASAL PFB-06. This research made use of APLpy, an open-source plotting package for Python (Robitaille and Bressert, 2012). This paper makes use of the following ALMA data: ADS/JAO.ALMA#2015.1.01013.S.

## References

- Bolato A. D., et al., 2008, ApJ, 686, 948
- Bolato A. D., Wolfire M., Leroy A. K., 2013, ARA&A, 51, 207
- Chen C. H. R., et al., 2014, ApJ, 785, 162
- Eckart A., et al., 1990, ApJ, 348, 434
- Gardiner L. T., Sawa T., Fujimoto M., 1994, MNRAS, 266, 567
- Harries T. J., Hilditch R. W., Howarth I. D., 2003, MNRAS, 339, 157
- Hindman J. V., Kerr F. J., McGee R. X., 1963, Australian Journal of Physics, 16, 570
- Larson R. B., 1981, MNRAS, 194, 809
- Lehner N., et al., 2008, ApJ, 678, 219
- MacLaren I., Richardson K. M., Wolfendale A. W., 1988, ApJ, 333, 821
- Mizuno N., et al., 2006, ApJ, 643, L107
- Muller E., et al., 2003, MNRAS, 339, 105
- Rubio M., et al., 2015, Nature, 525, 218
- Schruba A., et al., 2017, ApJ, 835, 278
- Solomon P. M., et al., 1987, ApJ, 319, 730
- Wong T., et al., 2011, ApJS, 197, 16